FULLY CONSTRAINED LEAST SQUARES LINEAR SPECTRAL UNMIXING OF *THE SCREAM* (*VERSO*, 1893)

Hilda Deborah

Department of Computer Science, Norwegian University of Science and Technology, Gjøvik, Norway

Magnus Orn Ulfarsson, Jakob Sigurdsson

Department of Electrical and Computer Engineering, University of Iceland Reykjavik, Iceland

ABSTRACT

Taking insights from the remote sensing field, in the recent decade, the advantages of hyperspectral imaging technology has been exploited for painting conservation. The estimation of pigment proportion in painting is a challenge that is due to the highly mixed nature of the paint layers, usually requiring to take into account the law of mixing colorants in turbid media. Having knowledge of some pigments and paint layers of the reverse side of *The Scream* (1893), in this study, we are exploring the feasibility of using a more simple linear model for its unmixing. The obtained results are promising, despite the simplicity of the mathematical model.

***Index Terms*—** hyperspectral images, spectral unmixing, fully constrained least squares, cultural heritage application

1. INTRODUCTION

The identification of an artist's material of a painting is traditionally carried out using micro-destructive techniques, e.g., X-ray fluorescence (XRF) and Fourier-transform infrared spectroscopy (FTIR) [1]. Despite allowing to identify pigments, dyes, and organic components present in the painting, they are only point-analysis. Hyperspectral imaging (HSI), which captures both spatial and spectral information, offers a complementary non-invasive technique to the field of conservation. With the characteristic wavelengths of paints lying in the visible and near-infrared spectral ranges [2], HSI can provide an analysis of pigments for the surface of a painting.

The use of spectral imaging for painting conservation started in the early 90s [3], aimed at providing more accurate documentation of cultural heritage paintings. In the recent decade, we can find works exploiting the use and advantages of HSI to provide, e.g., pigment and constituent maps, showing their presence [4] and also their estimated proportion or concentration in a mixture [5, 6]. From a computational point of view, these works can be categorized as classification or unmixing tasks. A classification task is when the aim is to identify the main pigments present in a painting. If the estimation of their proportion is also required, then the task becomes that of an unmixing.

Hyperspectral unmixing (HU) is an active research area in the field of remote sensing. It formulates that an observed spectral signature, typically originating from a single pixel, is of either micro- or macroscopic material mixtures and multiple scattering [7]. In remote sensing, due to the low resolution of the sensor, linear HU can be used since a macroscopic fashion (optical) of the mixture can be assumed. In painting conservation, the resolution of a pixel is very high, since the distance between the object of interest and the sensor is significantly closer compared to that in the remote sensing setup. Additionally, the mixing law for when different wet paints are mixed is different from that of an optical mixing in the atmosphere. Kubelka-Munk (K-M) theory is the mixing law of colorants that are largely used in the HU of paintings [5, 6].

K-M theory expresses the relationship between absorption and scattering coefficients of incident lights in intensely light scattering materials or, what is called, turbid media [8]. However, it is mathematically complex, making it unsuitable for many applications. This has lead to its simplifications which, nevertheless, still have their challenges. They are known to be restrictive and their shortcomings and limitations have also been identified [9, 10].

For paintings that have been previously analyzed using the traditional point-wise techniques, we have what is analogous to *ground truth* in the remote sensing context. This is available for *The Scream* (1893) by Edvard Munch [11, 12], for which we have also previously mapped the presence of its main pigments on the entire surface of the painting [4]. Exploiting the knowledge of the particular characteristics of its reverse side, in this study, we are exploring the feasibility of using the linear spectral mixture analysis approach. Details of the said characteristics, the methods, and our justification of its use can be found in Section 2. Some experimental results and analysis can be found in Section 3, followed by a conclusion in Section 4. Frequently used mathematical notations are also provided for ease of reading in Table 1.

This work is supported by FRIPRO FRINATEK Metrological texture analysis for hyperspectral images (projectnr. 274881) funded by the Research Council of Norway.

Table 1: Frequently used mathematical notations.

$\mathbf{Y}$	Image vector $\mathbf{Y} = [\mathbf{y}_p^T]$, $\mathbf{Y} \in \mathbb{R}_+^{P \times M}$, where $\mathbf{y}_p \in \mathbb{R}_+^{M \times 1}$ is the spectrum at pixel p
$\mathbf{A}$	Spectral signatures of known pigments $\mathbf{A} = [\mathbf{a}_r]$, $\mathbf{A} \in \mathbb{R}_+^{M \times R}$, $\mathbf{a}_r \in \mathbb{R}_+^{M \times 1}$
$\mathbf{S}$	Proportion vector $\mathbf{S} = [\mathbf{s}_p]$, $\mathbf{S} \in \mathbb{R}_+^{P \times R}$, $\mathbf{s}_p \in \mathbb{R}_+^{1 \times R}$
$\mathbf{1}_r, \mathbf{1}_p$	Vector of ones of size $R \times 1$ and $P \times 1$
M	Number of spectral bands
$P,\ p$	Number of pixels and pixel index
$R,\ r$	Number of known pigments and their index

2. MATERIALS AND METHODS

2.1. Target painting

The target painting for this study is the reverse side (*verso*) of the painted version of *The Scream* (tempera/ crayon/ oil, Woll 333) from 1893, owned by the National Museum of Art, Architecture and Design (NM) in Oslo, Norway [13]. Due to the size of the painting and the acquisition setup, the painting had to be scanned as three overlapping cutouts (Fig. 1). After a preprocessing, each cutout is of varying widths and heights around 1400×4680 pixels. Spectrally, it has 160 bands from approximately 414.62 to 992.50 nm, in 3.63 nm intervals. Due to the noise level at the first five bands, only 155 spectral bands starting from 432.80 nm are considered.

In an interview with a conservator from the NM [14], it was mentioned that Munch very rarely mixed the paints in the palette, but rather directly onto the cardboard support of this painting. It was further explained the technique he often used was brushing one paint thinly across another, resulting in a third color that is optically mixed. And as what can also be observed in the reverse side of the painting in Fig. 1, there are many strokes of clean or unmixed colors. There are also what is called the *scumble effects*, i.e., a perceptual effect that is due to the translucent colors lying across each other. Another important aspect of the painting that will be useful in the unmixing task is the cardboard support. It was said that there was no proper preparation for the cardboard. There is no ground layer aside from gelatin that was already on the cardboard itself. This means that for a thin layer of paint or pigment, the spectral reflectance will be that of an optical mixing with the reflectance of the cardboard support.

2.2. Fully constrained least squares unmixing

The characteristics of *The Scream* (1893), i.e., with many clean colors and scumble effects, justify the use of a more simple unmixing algorithm, i.e., fully constrained least squares (FCLS) linear spectral unmixing. In order to use the algorithm, *a priori* knowledge of the signatures of pigments present in the painting is required. In this case, this information is obtained from previous studies, where the main pigments have been identified in several points of the painting [11, 12]. Using them as guidance, spectral reflectances of the identified pigments can therefore be extracted from the hyperspectral image in order to build a matrix $\mathbf{A}$ containing the signatures of the pigments.

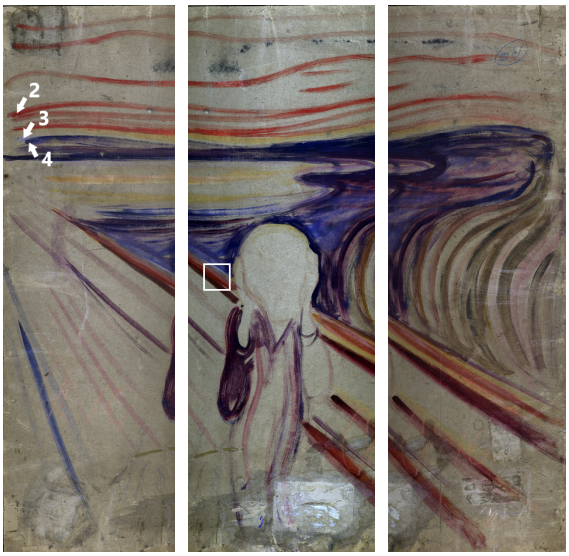

Fig. 1: Three hyperspectral cutouts of the reverse side (*verso*) of The Scream (1893).

For a linear unmixing approach to provide reliable and directly interpretable estimation of pigment proportion $\mathbf{S}$, two constraints must be imposed. They are the abundance non-negativity (ANC) and sum-to-one (ASC) constraints [15],

$$s_{pr} \geq 0,\ 1 \leq r \leq R; \quad \sum_{r=1}^{R} s_{pr} = 1.$$

These constraints allow embedding the physical aspects of materials into the algorithm. ANC says that the estimated proportion for each pigment must be a positive fraction, while ASC makes sure that the cumulative proportion of a single-pixel p does not go above 100%.

In a least squares linear unmixing, we consider a pixel $\mathbf{y}_p$ to be modeled as a linear combination of spectral signatures of known pigments $\mathbf{A}\mathbf{s}_p$ and an additive noise term ϵ_p,

$$\mathbf{y}_p = \mathbf{A}\mathbf{s}_p + \epsilon_p, \quad p = 1, \ldots, P.$$

Then, consider the optimization problem,

$$J = \min_{\mathbf{S}} \frac{1}{2} \sum_{p=1}^{P} \|\mathbf{y}_p - \mathbf{A}\mathbf{s}_p\|^2 + \lambda_1 \|\mathbf{S}\mathbf{1}_r - \mathbf{1}_p\|^2 + \lambda_2 \|\mathbf{S}\|_q,$$

$$\text{where } \|\mathbf{S}\|_q = \sum_{p=1}^{P} \sum_{r=1}^{R} s_{pr}^q,\ 0 < q < 1.$$

The first term in J enforces fidelity, the second encourages ASC, and the third acts as a sparsity term. Considering the whole image vector $\mathbf{Y}$, the function can be written as,

$$J = \min_{\mathbf{S}} \frac{1}{2}\|\mathbf{Y} - \mathbf{S}\mathbf{A}^T\|_F^2 + \lambda_1\|\mathbf{S}\mathbf{1}_r - \mathbf{1}_p\|^2 + \lambda_2\|\mathbf{S}\|_q.$$

To optimize J, the steepest descent method will be used, where its derivative w.r.t $\mathbf{S}$ is,

$$\frac{\partial J}{\partial \mathbf{S}} = \mathbf{S}\mathbf{A}^T\mathbf{A} - \mathbf{Y}\mathbf{A} + \lambda_2 q\|\mathbf{S}\|_{q-1} + \lambda_1\mathbf{S}\mathbf{1}_r\mathbf{1}_r^T - \lambda_1\mathbf{1}_p\mathbf{1}_r^T.$$

The (element-wise) steepest descent method for each iteration k is given by,

$$s_{pr}^{(k+1)} = s_{pr}^{(k)} - \eta_{pr}^{(k)}[(\mathbf{S}^{(k)}\mathbf{A}^T\mathbf{A})_{pr} - (\mathbf{Y}\mathbf{A})_{pr} + \lambda_2 q(s_{pr}^{(k)})^{q-1} + \lambda_1(\mathbf{S}^{(k)}\mathbf{1}_r\mathbf{1}_r^T)_{pr} - \lambda_1].$$

The step size η_{pr} is allowed to change at each k,

$$\eta_{pr}^{(k)} = \frac{s_{pr}^{(k)}}{[(\mathbf{S}^{(k)}\mathbf{A}^T\mathbf{A})_{pr} + \lambda_2 q(s_{pr}^{(k)})^{q-1} + \lambda_1(\mathbf{S}^{(k)}\mathbf{1}_r\mathbf{1}_r^T)_{pr}]}.$$

Finally, the update rule can be written as,

$$s_{pr}^{(k+1)} = \frac{s_{pr}^{(k)}[(\mathbf{Y}\mathbf{A})_{pr} + \lambda_1]}{[(\mathbf{S}^{(k)}\mathbf{A}^T\mathbf{A})_{pr} + \lambda_2 q(s_{pr}^{(k)})^{q-1} + \lambda_1(\mathbf{S}^{(k)}\mathbf{1}_r\mathbf{1}_r^T)_{pr}]}.$$

With regards to ANC, it is possible to show that the sequence of cost function values this algorithm yield is non-negative [16]. Note that the method relates to refs. [16, 17], written for non-negative matrix factorization setting.

2.3. Spectral library of pure and mixed pigments

Information of the main pigments present in the three locations pointed by white arrows in Fig. 1 is available [11]. Details of their corresponding pigments are provided in Table 2. Additionally, knowing that most of the surfaces are not covered by pigments, a signature of the cardboard support will also be used in the spectral library. Finally, spectral reflectances of these four samples are obtained from, first, averaging a 2×2 window and, then, smoothing them using Savitzky-Golay filter [18] of window length 7 and polynomial order 2. The resulting spectral library can be seen in Fig. 2.

3. RESULTS AND DISCUSSION

3.1. Evaluation using subsets containing the samples

To evaluate the feasibility of using FCLS for this painting, a subset of size 300×300 pixels is used, as well as the following tuning parameters $\lambda_1 = 1300, \lambda_2 = 23, q = 0.5$. It contains the location of the samples in Fig. 1. Closely observing the subset through Fig. 3a, it is almost certain that pure and/ or mixed pigments in this subset are only variations of samples 1-4. The estimated proportion in different pixels will vary, but no other pigments are expected on the surface, which will contribute to a significantly larger reconstruction error $e = \|\mathbf{Y} - \mathbf{S}\mathbf{A}^T\|_F^2$.

Table 2: Known pigments used in this study. Sample numbers in parentheses correspond to physical samples studied and analyzed in Ref. [11].

Sample	Colour	Main pigments found
1	-	Cardboard support
2 (33)	Red	Vermilion
3 (35)	White	LW mixture: Lead white, zinc white
4 (34)	Blue	UB mixture: Ultramarine blue, lead white, barites

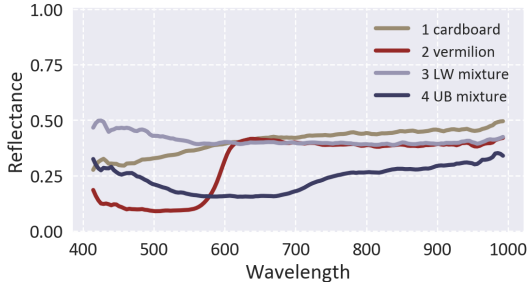

Fig. 2: Spectral reflectances of the samples given in Table 2. Colors of the spectra are representative of the main pigments.

The unmixing results can be observed in Fig. 3. The proportion maps for each sample in Fig. 3c-3f provide reasonable results agreeing with a quick visual observation on the target image. The map for the cardboard support (Fig. 3c) correctly shows where the cardboard is exposed, without any superposing paint layer. Its combination with the vermilion map (Fig. 3d) is also able to show where the vermilion layer is thinner and more translucent, showing the cardboard layer beneath. The map for the LW mixture correctly provides a high proportion in the brushstroke where sample 3 was taken from. However, it also shows that the LW mixture is found where the cardboard support is supposedly exposed. This can be explained through the high similarity between spectral reflectances of sample 1 (cardboard) and 3 (LW mixture), see Fig. 2. This is understandable and expected since in the VNIR spectral range, the shape of cardboard and white pigments spectra are difficult to differentiate. It can be easily solved by incorporating SWIR spectral ranges encompassing cellulose absorption bands.

Fig. 3f shows a high proportion of UB mixture in the brushstrokes area where sample 4 was taken from. However, this area also generates relatively high e in Fig. 3b. The spectra of three pixels with the highest e from this area are shown in Fig. 5. The spectrum corresponding to $e = 0.35$ has a

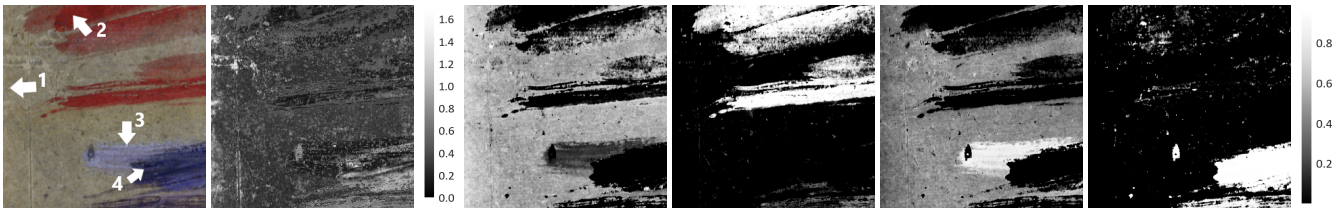

(a) Target subset (b) Reconstruction error (c) Cardboard (d) Vermilion (e) LW mixture (f) UB mixture

Fig. 3: Results for a subset of *verso* (L) containing the origin of samples 1–4 (Table 2). Subfigures (c)-(f) provide the estimated proportion of each samples and are of identical dynamic ranges, i.e., 0–1.

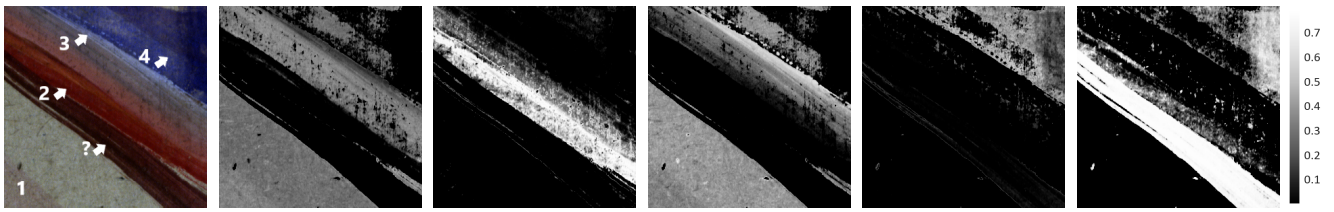

(a) Target subset (b) Cardboard (c) Vermilion (d) LW mixture (e) UB mixture (f) Unknown mixture

Fig. 4: Results for a subset containing paint layers supposedly of the samples in Table 2 and another unknown mixture.

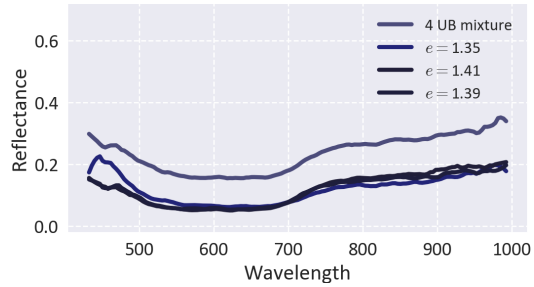

Fig. 5: Three pixels with highest reconstruction error e, located in brushtroke areas with high proportion of UB mixture.

peak at around 450 nm, which does not exist in the signature of sample 4 (UB mixture). This could mean that there is an unknown blue pigment in the mixture. The two other spectra are almost identical in shape with the spectrum of sample 4, only lower in intensity. FCLS deems them to be composed of nearly 100% sample 4. The reconstruction error is then due to the ASC constraint imposed on the algorithm. To go very close to the spectrum of sample 4, it would require $s_{pr} \geq 1$.

3.2. Unmixing of image subset of unknown paint layers

Using the knowledge from a previous mapping study [4], another subset is chosen as a target. Its location is approximately within the white square of the second image in Fig. 1. From that study we know that this subset contains vermilion and UB mixture. From a visual observation of Fig. 4a, it is possible that LW mixture is also present. Our hypothesis of where these known pigments are present are annotated in the target image. There is also an unknown red-brownish paint layer which was not recognized as vermilion in Ref. [4], giving a higher e compared to the rest. A quick experiment using only the spectral library in Table 2 also supports the mapping study.

Adding a signature of the unknown layer to the spectral library, the unmixing is carried out, resulting in maps in Fig. 4. As previously, the proportion map for cardboard (Fig. 4b) is able to identify the exposed support and where the paint layer above it is thin and translucent. The map for vermilion (Fig. 4c) agrees with the result in Ref. [4]. The issue with the LW mixture being recognized where the cardboard is exposed remains a challenge for this subset. However, the map (Fig. 4d) shows a high proportion of the mixture in a location agreeing with our hypothesis. The map for the UB mixture (Fig. 4e) also agrees with the result in Ref. [4], except for areas where the mixture is darker in color. Finally, for the unknown mixture, the map is giving nearly 100% in the brushstroke area where the signature is taken from. It also says that the top right area of the subset consists of this red-brownish pigment, which is likely a false-positive since it would most probably be a UB mixture [4]. This problem can be attributed to the use of F-norm in the cost function, which takes into account intensity differences between spectra while neglecting the shape information [19]. Intensity difference is necessary to calculate the proportion, however, shape difference captures the characteristics of individual pigments. For example, a mixture of red pigments would not typically have a peak around 450 nm, since it is usually the characteristic of blue pigments. This information of peak location will be well

accounted for in the shape difference, instead of the intensity.

4. CONCLUSION AND FUTURE WORK

The hyperspectral unmixing of paintings into their pigments is a challenge due to the complex nature of spectral mixing in turbid media, e.g., paint layers. Kubelka-Munk colorant mixing law is typically incorporated in the model. However, it is mathematically complex and its simplifications are also known to be restrictive. The reverse side of *The Scream* (1893) is composed of many clean colors and scumble effect, enabling us to assume that the painting can be modeled using a fully-constrained least-squares linear mixing model. A spectral library of known pigments was also built using a few *ground truth* information available from previous studies.

The results obtained in this study are promising, agreeing with a previous pigment mapping study. A number of limitations have been identified, suggesting some improvements for future works. A separate study can be carried out to build an optimal spectral library, guided by the knowledge of the available ground truth. More signatures of pigments beyond the ground truth would also be necessary, possibly using information from the front side of the painting. It would also be interesting to compare the results with an algorithm that uses, e.g., spectral angle distance in place of the F-norm, in order to account for individual pigment characteristics. Finally, a comparison with the widely used Kubelka-Munk theory would be necessary to provide more understanding of when a simpler mixing model can be employed for the unmixing of paintings.

5. REFERENCES

[1] V. Antunes, V. Serrão *et al.*, "Characterization of a pair of Goan paintings from the 16th-17th centuries," *Eur Phys J Plus*, vol. 134, no. 6, p. 262, 2019.

[2] M. T. Eismann, *Hyperspectral remote sensing*. SPIE, 2012.

[3] K. Martinez, "High resolution digital imaging of paintings: The Vasari Project," *Microcomputers for Information Management*, vol. 8, no. 4, pp. 277–283, 1991.

[4] H. Deborah, S. George, and J. Hardeberg, "Spectral-divergence based pigment discrimination and mapping: A case study on The Scream (1893) by Edvard Munch," *J. Am. Inst. Conserv.*, vol. 58, no. 1-2, pp. 90–107, 2019.

[5] F. M. Abed and R. S. Berns, "Linear modeling of modern artist paints using a modification of the opaque form of KubelkaMunk turbid media theory," *Color Res Appl*, vol. 42, no. 3, pp. 308–315, 2017.

[6] A. M. N. Taufique and D. W. Messinger, "Hyperspectral pigment analysis of cultural heritage artifacts using the opaque form of Kubelka-Munk theory," in *Algorithms, Technologies, and Applications for Multispectral and Hyperspectral Imagery XXV*, vol. 10986. SPIE, 2019, pp. 297–307.

[7] J. M. Bioucas-Dias, A. Plaza *et al.*, "Hyperspectral unmixing overview: Geometrical, statistical, and sparse regression-based approaches," *IEEE J Sel Top Appl Earth Obs Remote Sens*, vol. 5, no. 2, pp. 354–379, 2012.

[8] H. Yang, S. Zhu, and N. Pan, "On the Kubelka-Munk single-constant/two-constant theories," *Text Res J*, vol. 80, no. 3, pp. 263–270, 2010.

[9] R. S. Berns and M. Mohammadi, "Single-constant simplification of Kubelka-Munk turbid-media theory for paint systems–A review," *Color Res Appl*, vol. 32, no. 3, pp. 201–207, 2007.

[10] A. K. R. Choudhury, "Instrumental colourant formulation," in *Principles of Colour and Appearance Measurement*. Woodhead Publishing, 2015, pp. 117–173.

[11] B. Singer, T. E. Aslaksby *et al.*, "Investigation of materials used by Edvard Munch," *Stud Conserv*, vol. 55, no. 4, pp. 274–292, 2010.

[12] I. C. A. Sandu, T. Ford *et al.*, "The "Scream" by Edvard Munch - Same motif, different colours, different techniques and approaches – A novel non-invasive comparative study of two of its versions," in *5th International Congress on Chemistry for Cultural Heritage (ChemCH2018)*, 2018.

[13] T. E. Aslaksby, "Edvard Munch's painting The Scream (1893): Notes on technique, materials and condition," in *Public paintings by Edvard Munch and some of his contemporaries. Changes and conservation challenges.* Archetype Publications, 2015.

[14] Exhibition on Screen. (2017) Interview with Trond E. Aslaksby, Conservator, The National Museum in Oslo. https://www.youtube.com/watch?v=5QpwoNXel6E.

[15] D. C. Heinz and C. I. Chang, "Fully constrained least squares linear spectral mixture analysis method for material quantification in hyperspectral imagery," *IEEE Trans Geosci Remote Sens*, vol. 39, no. 3, pp. 529–545, 2001.

[16] Y. Qian, S. Jia *et al.*, "Hyperspectral unmixing via $L_{1/2}$ sparsity-constrained nonnegative matrix factorization," *IEEE Trans Geosci Remote Sens*, vol. 49, no. 11, pp. 4282–4297, 2011.

[17] D. D. Lee and H. S. Seung, "Algorithms for non-negative matrix factorization," in *Proc. 13th International Conference on Neural Information Processing Systems*, 2000, pp. 535–541.

[18] A. Savitzky and M. J. E. Golay, "Smoothing and differentiation of data by simplified least squares procedures," *Anal. Chem*, vol. 36, no. 8, pp. 1627–1639, 1964.

[19] H. Deborah, N. Richard, and J. Y. Hardeberg, "A comprehensive evaluation of spectral distance functions and metrics for hyperspectral image processing," *IEEE J Sel Top Appl Earth Obs Remote Sens*, vol. 8, no. 6, pp. 3224–3234, 2015.